Pergamon

Int. J. Heat Mass Transfer. Vol. 39, No. 2, pp. 383–390, 1996

0017-9310/96 $9.50+0.00

0017-9310(95)00130-1

Numerical simulation for conjugate problem of natural convection on both sides of a vertical wall

HAN-TAW CHEN and SHIUH-MING CHANG

Department of Mechanical Engineering, National Cheng Kung University, Tainan, Taiwan, 701, Republic of China

(*Received* 6 *September* 1994 *and in final form* 15 *December* 1994)

Abstract—The present analysis is presented to predict the heat transfer rate between two natural convection systems at different temperatures separated by a vertical plate, where the effects of one-dimensional heat conduction along the plate and transverse heat conduction will be discussed. Thus, the countercurrent boundary layer flow is formed on the two sides. Governing boundary layer equations with their corresponding boundary conditions for these two natural convection systems are cast into dimensionless forms by using the non-similarity transformation. The resulting system of equations is solved by using the finite difference approximation for the heat conduction equation and the local non-similarity method in conjunction with the Nachtsheim–Swigert iteration scheme for boundary layer equations. Excellent agreement between the present results predicted by using the approximation of heat conduction along the plate and reliable experimental data is obtained. This implies that the present analysis provides accurate prediction for such problems.

INTRODUCTION

The heat transfer mode across a vertical wall separating two semi-infinite fluid reservoirs at different temperatures has great practical importance in numerous thermal engineering applications [1]. Various numerical methods have been proposed to analyze such problems [1–6]. Lock and Ko [2] analyzed the problem of thermal interaction through a wall between two free convective systems using the concept of local similarity and the method of integration. In their study, the effect of plate resistance was not negligible. Anderson and Bejan [3] also investigated the similar problem. However, the value of the fluid Prandtl number, *Pr*, was assumed to approach infinity. Accordingly, they applied the modified Oseen technique [7] to linearize the energy equation in the natural convection system. Furthermore, they constructed an analytical solution without making assumptions about the heat flux or temperature distribution at the wall. An important conclusion in this study [3] was that the vertical wall can be approximated as a constant heat flux surface and that the overall heat transfer rate is relatively independent of *Pr* provided *Pr* was $\leqslant 1$. Afterward, they also applied the similar technique to investigate problems with two fluid-saturated porous reservoirs at different temperatures [4] and a porous reservoir and a fluid reservoir at different temperatures [5]. Faghri and Sparrow studied the conjugate problem of thin film condensation on the outside of a vertical pipe and the fully developed forced convection of the cold fluid inside the pipe using a simple analysis in conjunction with the Runge–Kutta scheme [8]. Viskanta and Abrams [1] studied the problem of heat exchange between two forced convection systems separated by a plate. They presented a general analysis for cocurrent and countercurrent, laminar or turbulent flow. In addition, Viskanta and Lankford [9] also applied a simple analysis to investigate the thermal coupling of heat transfer between two natural convection systems separated by a vertical wall of 10.16 cm high and 0.635 cm thick. In this work [9], they assumed that heat conduction along the plate was negligible in comparison to transverse heat conduction. It can be found from their results [9] obtained by iteration using 20, 40 and 100 intervals $\Delta\xi_1$ for ξ_1 between 0 and 1, that the difference between the calculated and measured surface temperatures was greatest near both the ends. They [9] thought that this discrepancy was primarily attributed to the two-dimensional (2D) heat conduction effects in the plate or was due to the finite size of the two chambers.

The present study proposes a mathematical model to investigate the conjugate problem of natural convection on both sides of a vertical wall problem, which has been studied by Lock and Ko [2], Anderson and Bejan [3] and Viskanta and Lankford [9]. To obtain the more accurate predicted result of such a problem, the 2D heat conduction effects in the plate should be considered. However, the approximation of the 1D heat conduction along the vertical plate is taken into account because the aspect ratio (thickness/height) t/L is sufficiently small in this study. To the authors' knowledge, the predicted results obtained by using the approximation of the 1D heat conduction along the plate have not yet been found in the literature. Furthermore, the differences of the surface temperature and local Nusselt number along the vertical plate on

NOMENCLATURE

- A thermal resistance ratio, equation (18)
- B constant
- f_i reduced stream function
- g_a gravitational acceleration
- h_{x1}, h_{x2} local heat transfer coefficients
- k thermal conductivity
- L height of plate
- Nu_2 Nusselt number for the cold fluid, equation (29)
- Nu_{x2} local Nusselt number for the cold fluid, equation (26)
- Pr_i Prandtl number
- q_{x2} local heat flux through the the plate facing the cold reservoir
- Q_2 total heat flux through the the plate, equation (27)
- Ra_i Rayleigh number, equation (4)
- Ra_{x2} local Rayleigh number
- R_t, R_t^* thermal resistance ratios, equations (19) and (22)
- t thickness of plate
- T_i fluid temperature in the ith reservoir
- T_w plate temperature
- T_{wi} plate temperature facing the ith reservoir
- u, v velocity components in x- and y-directions
- $\tilde{u}, \tilde{v}$ dimensionless velocity components in x- and y-directions, equation (4)
- x_1, y_1 Cartesian coordinates, Fig. 1
- x_2, y_2 Cartesian coordinates, Fig. 1
- y_1^*, y_2^* dimensionless horizontal coordinates, equation (4).

Greek symbols

- α_i thermal diffusivity
- β_i coefficient of thermal expansion for the ith fluid
- θ_i dimensionless fluid temperature, equation (4)
- θ_w dimensionless plate temperature, equation (5)
- θ_{wi} dimensionless plate temperature facing the ith reservoir, equation (5)
- v_i kinematic viscosity
- ξ_1, ξ_2 dimensionless coordinates, equation (4)
- η_1, η_2 dimensionless parameters, equation (7)
- ψ_i stream function, equation (7).

Subscripts

- 1, 2, i hot, cold, ith fluid
- ∞ ambient condition
- w at the plate.

the cold reservoir obtained by using the approximation of transverse heat conduction and 1D heat conduction along the plate are also investigated for various important parameters in this problem. Due to close coupling for this system, all the boundary layer equations on the two sides and the 1D heat conduction equation for the vertical plate must simultaneously be solved by using the two-equation model of the local non-similarity method [10] and the finite-difference approximation. The main purpose of the present study is to investigate the accuracy of the predicted results obtained by using the approximation of the 1D heat conduction along the plate. Thus its predicted results compare with experimental data obtained by Viskanta and Lankford [9]. In addition, the effects of the Prandtl number on the cold reservoir Pr_2, the thermal resistance ratios R_t and A on the heat transfer rate between two convection systems will also be illustrated. It is worth mentioning that neither the surface temperature nor the heat flux through the plate is known *a priori*. Thus an iterative procedure would have to be applied.

MATHEMATICAL FORMULATION

The physical model of this study with the coordinate system is schematically shown in Fig. 1. The experiments of this study have been made by Viskanta and Lankford [9]. In this study, a vertical impermeable plate separates two semi-infinite fluid reservoirs at different temperatures. $T_{1\infty}$ and $T_{2\infty}$ respectively denote the ambient temperatures in the hot and cold reservoirs, where $T_{1\infty}$ is assumed to exceed $T_{2\infty}$. Thus the cooling effect of the cold reservoir is felt from the hot reservoir through the vertical plate. At the same time, the heating effect of the hot reservoir gives rise

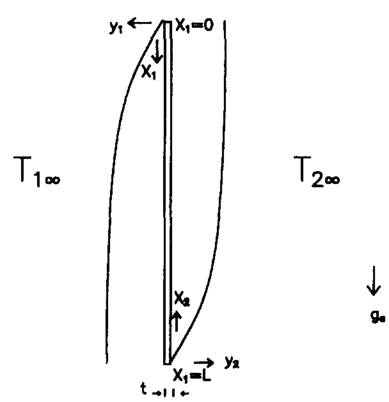

Fig. 1. Schematic representation of the system.

to an upward flow along the plate in the cold reservoir. The above statement implies that two fluid streams of this problem move in opposite directions. It is worth mentioning that this analysis is restricted to the case after steady-state conditions have been reached. In addition, it is also assumed that the flow is laminar and that physical properties are constant except the density in the buoyancy term. Based on the above assumptions, this problem can be formulated in terms of the boundary layer equations for two different fluid streams and heat conduction equation for the plate. It is evident that phenomenon of thermal coupling is produced by the conducting vertical plate separating two boundary layers.

The dimensionless form of the boundary layer equations expressing the conservation of mass, momentum and energy for two different fluid streams shown in Fig. 1 can respectively be written as

$$\frac{\partial \tilde{u}_i}{\partial \xi_i}+\frac{\partial \tilde{v}_i}{\partial y_i^*}=0 \tag{1}$$

$$\frac{1}{Pr_i}\left(\tilde{u}_i\frac{\partial \tilde{u}_i}{\partial \xi_i}+\tilde{v}_i\frac{\partial \tilde{u}_i}{\partial y_i^*}\right)=\theta_i+\frac{\partial^2 \tilde{u}_i}{\partial y_i^{*2}} \tag{2}$$

$$\tilde{u}_i\frac{\partial \theta_i}{\partial \xi_i}+\tilde{v}_i\frac{\partial \theta_i}{\partial y_i^*}=\frac{\partial^2 \theta_i}{\partial y_i^{*2}} \quad \text{for } i=1,2. \tag{3}$$

The dimensionless parameters in equations (1)–(3) are defined as

$$y_i^*=Ra_i^{1/4}y_i/L \quad \xi_1=x_1/L \quad \xi_2=x_2/L=1-\xi_1$$
$$\tilde{u}_i=u_iL/\alpha_iRa_i^{1/2} \quad \tilde{v}_i=v_iL/\alpha_iRa_i^{1/4} \quad Pr_i=v_i/\alpha_i$$
$$\text{and } \theta_i=|T_i-T_{i\infty}|/(T_{1\infty}-T_{2\infty}) \tag{4}$$

where Ra_i is the Rayleigh number for the ith fluid and is defined as $Ra_i=g_a\beta_i(T_{1\infty}-T_{2\infty})L^3/v_i\alpha_i$.

The corresponding boundary conditions are

$$\tilde{u}_i=\tilde{v}_i=0 \quad \theta_i=\theta_{wi}(\xi_i)(\text{or } \theta_i=\theta_w(\xi_i)) \quad \text{at } y_i^*=0 \tag{5}$$

$$\tilde{u}_i=0 \quad \theta_i=0 \quad \text{as } y_i^*\to\infty \tag{6}$$

where $\theta_{wi}=|T_{wi}-T_{i\infty}|/(T_{1\infty}-T_{2\infty})$. T_{wi} denotes the plate temperatures facing the ith fluid. $\theta_w=(T_w-T_{2\infty})/(T_{1\infty}-T_{2\infty})$. Only the boundary condition of $\theta_i=\theta_{wi}(\xi_i)$ at $y_i^*=0$ is given provided heat conduction along the vertical plate is neglected. However, if the 1D heat conduction along the plate is considered, only the boundary condition of $\theta_i=\theta_w(\xi_i)$ at $y_i^*=0$ will be assumed.

To apply the two-equation model of the local non-similarity method [10] to solve the present problem, the dimensionless variable η_i and reduced stream function f_i are first introduced:

$$\eta_i=y_i^*/\xi_i^{1/4} \quad \psi_i=f_i(\xi_i,\eta_i)\xi_i^{3/4}. \tag{7}$$

It is evident that the stream function ψ_i can be obtained from the definition of $\tilde{u}_i=\partial\psi_i/\partial y_i^*$ and $\tilde{v}_i=-\partial\psi_i/\partial\xi_i$ which satisfies the continuity equation (1). Due to the introduction of the dimensionless parameters in equations (4) and (7), the remaining partial differential equations (2) and (3) can be transformed into their corresponding ordinary differential equations. The substitution of equations (4) and (7) into equations (2) and (3) can yield a set of the dimensionless forms.

$$f_i'''+[3f_if_i''/4-(f_i')^2/2]/Pr_i+\theta_i=\xi_i(f_i'g_i'-f_i''g_i)/Pr_i \tag{8}$$

$$\theta_i''+3f_i\theta_i'/4=\xi_i(f_i'\varphi_i-\theta_i'g_i) \tag{9}$$

where $g_i=\partial f_i/\partial\xi_i$ and $\varphi_i=\partial\theta_i/\partial\xi_i$. The primes denote differentiation with respect to η_i.

Two additional differential equations can be obtained by differentiating equations (8) and (9) with respect to ξ_i. To close the system of boundary layer equations at the second-order level, terms involving $\partial g_i/\partial\xi_i$ and $\partial\varphi_i/\partial\xi_i$ are ignored. Based on this assumption, these two additional differential equations can be expressed as

$$g_i'''+(3f_ig_i''/4+7g_if_i''/4-3f_i'g_i')/Pr_i+\varphi_i=\xi_i(g_i'^2-g_i''g_i)/Pr_i \tag{10}$$

$$\varphi_i''+3f_i\varphi_i'/4+7g_i\theta_i'/4-f_i'\varphi_i=\xi_i(g_i'\varphi_i-\varphi_i'g_i). \tag{11}$$

It is evident that equations (8)–(11) constitute a set of ordinary differential equations, parameterized in ξ_i. The whole set of boundary conditions is given as:

$$f_i=f_i'=g_i=g_i'=0, \quad \theta_i=\theta_{wi}(\text{or } \theta_i=\theta_w) \quad \text{at } \eta_i=0 \tag{12}$$

$$f_i'=g_i'=0, \quad \theta_i=0 \text{ and } \varphi_i=0 \quad \text{as } \eta_i\to\infty \tag{13}$$

where θ_{wi} and θ_w are not known *a priori*.

The 2D heat conduction equation with constant thermal properties for the plate can be expressed as

$$\frac{\partial^2 T_w}{\partial x_2^2}+\frac{\partial^2 T_w}{\partial y_2^2}=0. \tag{14}$$

Its corresponding boundary conditions are:

$$\frac{\partial T_w}{\partial x_2}=0 \text{ at } x_2=0,L \tag{15}$$

$$-k_w\frac{\partial T_w}{\partial y_2}=h_{x2}(T_w-T_{2\infty})=-k_2\frac{\partial T_2}{\partial y_2} \quad \text{at } y_2=0 \tag{16}$$

$$-k_w\frac{\partial T_w}{\partial y_2}=h_{x1}(T_{1\infty}-T_w)=k_1\left.\frac{\partial T_1}{\partial y_1}\right|_{y_1=0} \quad \text{at } y_2=-t \tag{17}$$

where L is the height of the plate, t is the thickness of the plate, k_w is the thermal conductivity of the plate, h_{x1} and h_{x2} are the local heat transfer coefficients for the hot and cold fluids, respectively.

The local heat transfer coefficients h_{x1} and h_{x2} to be used in the above heat conduction equation are the outcome of the solutions of the boundary layer equations, but the thermal boundary conditions corresponding to the boundary layer equations are the outcome of the solutions of the heat conduction equation.

If heat conduction along the plate is neglected in comparison to transverse heat conduction, the couplings between heat conduction and boundary layer equations can be expressed by using the requirements that the heat flux and temperature are continuous at the plate–fluid interfaces. The couplings can be obtained from equations (14), (16) and (17).

$$k_1 \frac{\partial T_1}{\partial y_1}\bigg|_{y_1=0} = \frac{k_w}{t}(T_{w1} - T_{w2}) = -k_2 \frac{\partial T_2}{\partial y_2}\bigg|_{y_2=0}. \tag{18}$$

The value of $\partial T_w/\partial x_2$ along the plate is assumed a constant value. Based on this assumption, the term $\partial^2 T_w/\partial^2 x_2$ in equation (14) can be neglected. However, due to the existence of the boundary condition (15), this constant value must be zero. This result will lead to the assumption of the constant wall temperature. It is found from ref. [9] that the measured natural convection heat transfer coefficients are a maximum of about 12% higher than those expected for a constant wall temperature. This implies that it is difficult to obtain a more accurate predicted result provided the assumption of the constant wall temperature is applied. If the boundary conditions at $x_2 = 0$ and L are regarded as singular, namely, the value of $\partial T_w/\partial x_2$ along the plate is not equal to zero except near its two ends, the wall temperature will increase almost linearly with height. As stated by Viskanta and Lankford [9], the wall heat flux is practically constant over about 80% of the central height for $A = 1$ and $Pr_1 = Pr_2$ even though the wall temperatures vary significantly with the distance along the plate. However, the variations of the wall heat flux near the top and the bottom of the plate are relatively large. The heat transfer coefficients predicted by using this assumption are about 5% higher than experimental data. Anderson and Bejan [3] were also of the opinion that the vertical plate can be approximated as a constant heat flux surface. The above statements imply that the approximation of transverse heat conduction has better accuracy than that of an isothermal wall temperature. However, it is worth mentioning that, near the two ends of the plate, the present boundary layer approximations break down, and the wall temperature departs from its linear distribution.

Substituting some dimensionless parameters in equation (4) and the definition of θ_{w2} and θ_{w1} into equation (18) yields

$$\theta_{w2} = \theta_{w1} - R_t \frac{\partial \theta_1}{\partial y_1^*}\bigg|_{y_1^*=0} \tag{19}$$

where R_t denotes the thermal resistance ratio of the plate to the boundary layer for the hot fluid and is defined as $R_t = (k_1/k_w)(t/L)Ra_1^{1/4}$.

The variation of the wall temperature distribution can be approximated by a 1D conducting system provided the aspect ratio t/L is sufficiently small. Based on this assumption, equation (14) can be simplified as

$$k_w t \frac{d^2 T_w}{dx_2^2} - h_{x1}(T_w - T_{1\infty}) - h_{x2}(T_w - T_{2\infty}) = 0. \tag{20}$$

Its corresponding boundary conditions of equation (20) are

$$\frac{dT_w}{dx_2} = 0 \text{ at } x_2 = 0, L. \tag{21}$$

Substituting equations (16) and (17) and some the relatively dimensionless parameters in equations (4) and (7) into equation (20) yields

$$\frac{d^2\theta_w}{d\xi_2^2} + R_t^* A(1-\xi_2)^{-1/4} \frac{\partial \theta_1}{\partial \eta_1}\bigg|_{\eta_1=0} + R_t^* \xi_2^{-1/4} \frac{\partial \theta_2}{\partial \eta_2}\bigg|_{\eta_2=0} = 0 \tag{22}$$

where A denotes the thermal resistance ratio for the two boundary layers and is defined as $A = (k_1/k_2)(Ra_1/Ra_2)^{1/4}$. R_t^* can be regarded as the thermal resistance ratio of the plate to the boundary layer for the cold fluid and is defined as $R_t^* = [(k_2/k_w)(t/L)Ra_2^{1/4}](L/t)^2 = R_t(L/t)^2/A$.

The differential form of equation (22) can be written as

$$\frac{\theta_{w,p-1} - 2\theta_{w,p} + \theta_{w,p+1}}{\Delta\xi_2^2} + R_t^* A(1-\xi_{2,p})^{-1/4}\theta_1'(1-\xi_{2,p}, \eta_1 = 0) + R_t^* \xi_{2,p}^{-1/4}\theta_2'(\xi_{2,p}, \eta_2 = 0) = 0 \quad \text{for } p = 1, 2, \ldots, N \tag{23}$$

where $\xi_{2,1} = 0$. N denotes the total nodal number in the vertical plate.

The local heat transfer coefficient h_{x2} for the cold fluid can be expressed as

$$h_{x2} = k_2 \frac{\partial T_2}{\partial y_2}\bigg|_{y_2=0} \Big/ [T_2(x_2, y_2 = 0) - T_{2\infty}] = -q_{x2}/[T_2(x_2, y_2 = 0) - T_{2\infty}] \tag{24}$$

where q_{x2} denotes the local heat flux through the plate facing the cold fluid and is defined as $q_{x2} = -k_2(\partial T_2/\partial y_2)|_{y_2=0}$.

The substitution of the dimensionless parameters in equation (4) into equation (24) yields the other expression of h_{x2} as

$$h_{x2} = -[\theta_2'(\xi_2, \eta_2 = 0)/\theta_{w2}]Ra_2^{1/4}k_2/(L\xi_2^{1/4}). \tag{25}$$

The local Nusselt number Nu_{x2} for the cold fluid can be expressed as

$$Nu_{x2} = \frac{h_{x2}x_2}{k_2} = -Ra_{x2}^{1/4}\theta_2'(\xi_2, \eta_2 = 0)/\theta_{w2}$$

or

$$Nu_{x2}/Ra_{x2}^{1/4} = -\theta_2'(\xi_2, \eta_2 = 0)/\theta_{w2}^{5/4} \qquad (26)$$

where Ra_{x2} is the local Rayleigh number for the cold fluid and is defined as $Ra_{x2} = g\beta(T_{w2} - T_{2\infty})x_2^3/\nu_2\alpha_2$.

The total heat flux Q_2 through the plate facing the cold fluid is obtained by integrating numerically q_{x2} over the entire height of the plate can be expressed as

$$Q_2 = -k_2 \int_0^L \left[\frac{\partial T_2}{\partial y_2}\bigg|_{y_2=0} \right] dx_2. \qquad (27)$$

It can be seen that the local heat flux q_{x2} is singular at $\xi_2 = 0$ and 1. However, the value of Q_2 is finite. Its value can be obtained by using the trapezoidal rule. The substitution of the dimensionless variables in equation (4) into equation (27) can obtain the dimensionless form of Q_2 as

$$\tilde{Q}_2 = \frac{Q_2}{k_2(T_{1\infty} - T_{2\infty})}$$

$$= -Ra_2^{1/4} \int_0^1 \theta_2'(\xi_2, \eta_2 = 0)/\xi_2^{1/4}\, d\xi_2$$

$$= BRa_2^{1/4} \qquad (28)$$

where $B = -\int_0^L \theta_2'(\xi_2, \eta_2 = 0)\, d\xi_2$.

Accordingly, the Nusselt number facing the cold fluid can be expressed as

$$Nu_2 = \tilde{Q}_2 = BRa_2^{1/4}. \qquad (29)$$

Solution procedure

All the computations are performed on the PC with an 80486 microprocessor. The present numerical results are obtained by using 51 nodes for the natural convection sides and nine nodes in the ξ_2-direction for the approximation of transverse heat conduction (or 25 nodes for the approximation of 1D heat conduction). The maximum number of iterations is about five times. The computational procedures of solving the present problem are listed in the following.

(1) The boundary layer equations (8)–(11) at $\xi_2 = \Delta\xi_2$, together with the boundary condition (12) and (13), are solved by using the fourth order Runge–Kutta method in conjunction with the Nachtsheim–Swigert iteration scheme [11] to fulfil the boundary conditions at the edge of the boundary layer for the natural convection sides. Otherwise, the entire calculation is repeated until the requirements at the plate are satisfied.

(2) The computational processes of step 1 are repeated by advancing in a small space-step $\Delta\xi_2$ until $\xi_2 = 1 - \Delta\xi_2$.

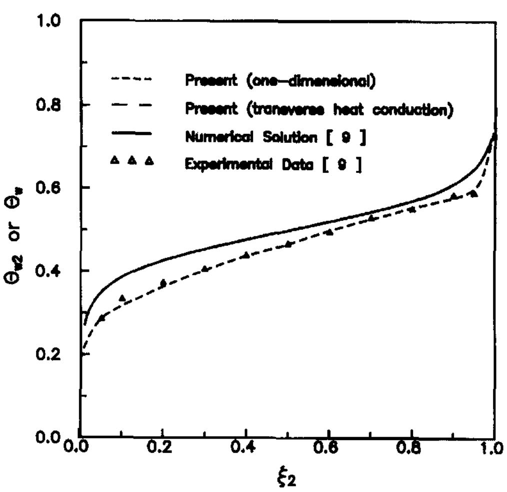

Fig. 2. Comparison of predicted and measured surface temperatures along the plate for $A = 1.01$ and $R_t = 0.000148$.

(3) The entire computational procedures are finished until the wall temperature distribution obtained from steps 1 and 2 is convergent.

RESULTS AND DISCUSSION

The predicted and measured surface temperatures [9] facing the cold reservoir are respectively compared in Figs. 2–4 for $Pr_1 = Pr_2 = 0.708$ and three different materials: glass, brass and copper. It can be found from Figs. 2 and 3 that the present predicted results using the approximation of transverse heat conduction are very close to those given by Viskanta and Lankford [9] for the copper and brass plates ($R_t = 0.000148$ and $R_t = 0.00103$). However, Fig. 4 shows that the present predicted results using the approximation of transverse heat conduction are closer to experimental data than those given by Viskanta and Lankford [9] for the glass plate

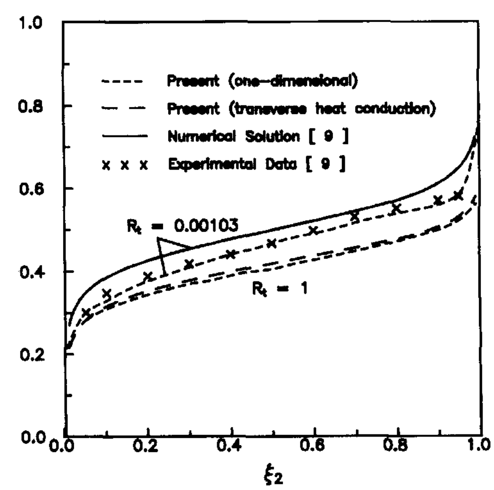

Fig. 3. Comparison of predicted and measured surface temperatures along the plate for $A = 0.997$ and various R_t values.

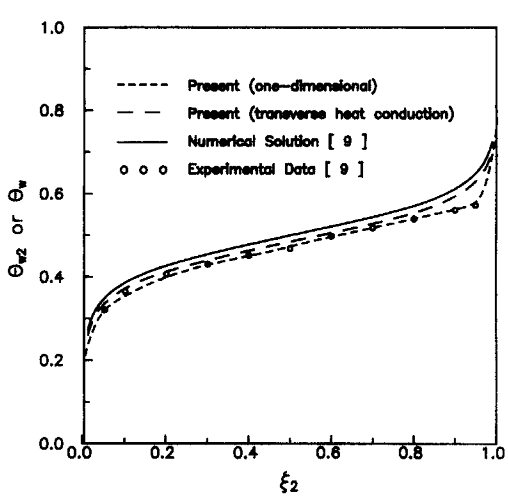

Fig. 4. Comparison of predicted and measured surface temperatures along the plate for $A = 0.97$ and $R_t = 0.0914$.

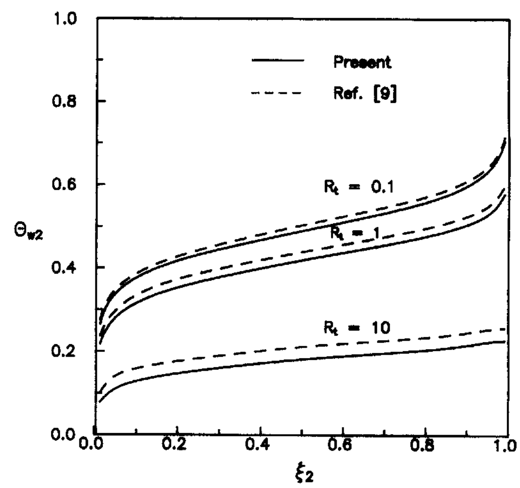

Fig. 6. Effect of R_t on θ_{w2} for $A = 1$ and $Pr_1 = Pr_2 = 0.708$.

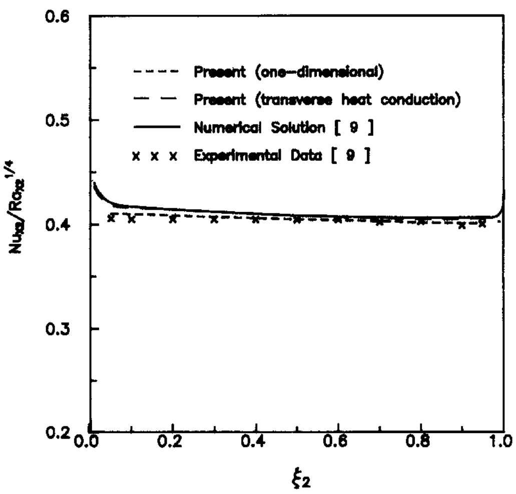

Fig. 5. Comparison of predicted and measured local Nusselt numbers for $A = 0.997$, $Pr_1 = Pr_2 = 0.708$ and $R_t = 0.00103$.

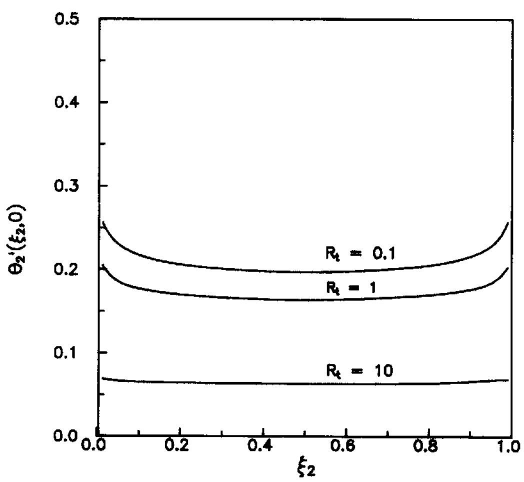

Fig. 7. Effect of R_t on $\theta_2'(\xi_2, 0)$ for $A = 1$ and $Pr_1 = Pr_2 = 0.708$.

($R_t = 0.0914$). It is worth mentioning that the predictions of Viskanta and Lankford [9] for the glass plate were very close to those for the copper and brass plates. At the same time, their calculated results [9] are equal to or higher than the present results. The engineering importance of this study is that the present predicted results using the approximation of 1D heat conduction along the plate are in good agreement with experimental data for copper, brass and glass plates even near the ends of the vertical plate. Figure 3 also shows that the difference of the dimensionless surface temperatures obtained by using the approximation of transverse heat conduction and 1D heat conduction along the plate lessens when the value of R_t increases.

The comparison of the predicted and measured local Nusselt numbers for $A = 0.997$ and $R_t = 0.00103$ is shown in Fig. 5. The present results using the approximation of transverse heat conduction are very close to those given by Viskanta and Lankford [9]. However, the measured experimental data are in good agreement with the present results using the approximation of 1D heat conduction and are lower than those given by Viskanta and Lankford [9]. This conclusion further proves that the present method with the approximation of 1D heat conduction has good accuracy for such problems.

The present predicted results shown in Figs. 6–9 and Table 1 are obtained by using the approximation of transverse heat conduction. The effect of R_t on the dimensionless surface temperature, θ_{w2}, and the dimensionless temperature gradient at $\eta_2 = 0$, $\theta_2'(\xi_2, 0)$, is shown in Figs. 6 and 7 for $A = 1$, $Pr_1 = Pr_2 = 0.708$ and various R_t values. The limiting case of $R_t = 0$ corresponds to a plate having no thermal resistance between the two boundary layers. For a fixed value of A, an increase in parameter R_t can increase the temperature difference across the plate. Thus an increase in R_t can yield a more uniform wall

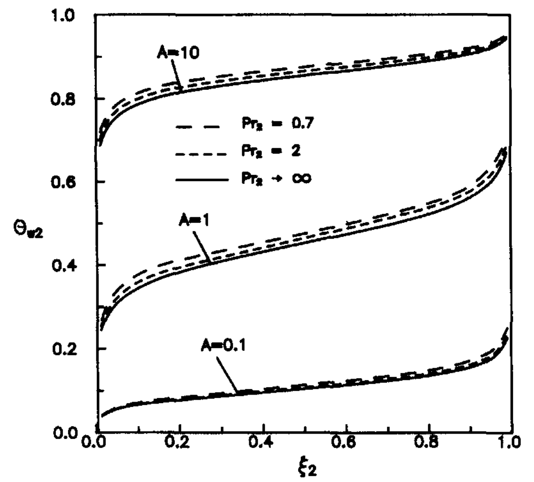

Fig. 8. Effect of A on θ_{w2} for $R_t = 0.1$, $Pr_1 = 0.7$ and various Pr_2 values.

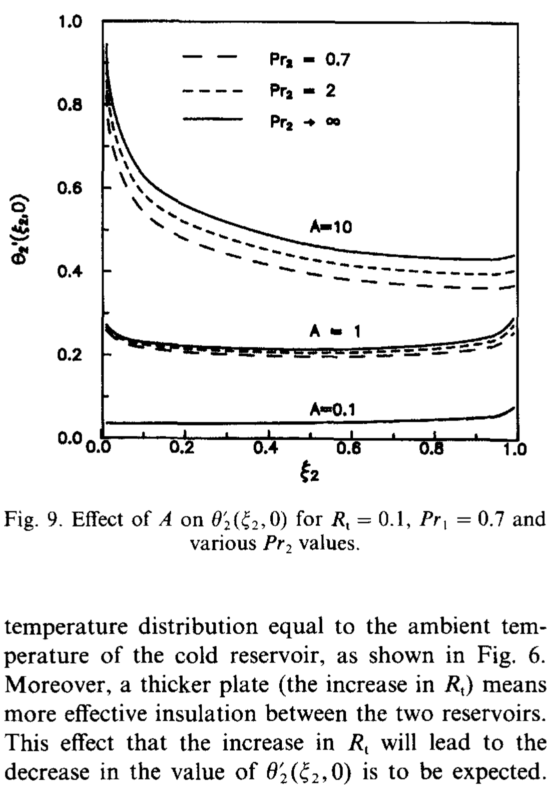

Fig. 9. Effect of A on $\theta_2'(\xi_2, 0)$ for $R_t = 0.1$, $Pr_1 = 0.7$ and various Pr_2 values.

temperature distribution equal to the ambient temperature of the cold reservoir, as shown in Fig. 6. Moreover, a thicker plate (the increase in R_t) means more effective insulation between the two reservoirs. This effect that the increase in R_t will lead to the decrease in the value of $\theta_2'(\xi_2, 0)$ is to be expected. Figure 6 also shows that the difference of θ_{w2} between the present predicted results and those given by Viskanta and Lankford [9] becomes great for $A = 1$ when the value of R_t increases, as shown in Fig. 3.

Table 1. Variation of Pr_2 with $Nu_2/Ra_2^{1/4}$ for $R_t = 0.1$, $Pr_1 = 0.7$ and various A values

	$Nu_2/Ra_2^{1/4}$		
Pr_2	$A = 10$	$A = 1$	$A = 0.1$
0.7	0.4427	0.2122	0.0422
2	0.4800	0.2222	0.0426
∞	0.5184	0.2309	0.0429

Figures 8 and 9 show the effect of the thermal resistance ratio for the two boundary layers A on θ_{w2} and $\theta_2'(\xi_2, 0)$ for $R_t = 0.1$, $Pr_1 = 0.708$ and various Pr_2 values. For $A < 1$, the resistance to heat transfer in the cold reservoir is much larger than that in the hot reservoir [9]. It is found that the effect of Pr_2 on θ_{w2} and $\theta_2'(\xi_2, 0)$ for $R_t = 0.1$, $Pr_1 = 0.708$ and $A \leqslant 0.1$ is negligible. Examining the physical significance of Pr_2 indicates that the thermal boundary layer thickness in the cold reservoir increases with decreasing Pr_2. This statement implies that θ_{w2} tends to the ambient temperature of the hot reservoir when Pr_2 decreases, as shown in Fig. 8. Thus decreasing Pr_2 tends to lower the heat transfer rate through the plate and leads to the decrease in $\theta_2'(\xi_2, 0)$. These phenomena can be found in Fig. 9. Figures 8 and 9 show that the effect of Pr_2 on θ_{w2} and $\theta_2'(\xi_2, 0)$ is considerably weaker than that of A. In addition, it can be found from Fig. 9 that the effect of Pr_2 on $\theta_2'(\xi_2, 0)$ can be neglected for $A < 1$. However, its effect is not negligible for $A = 10$.

The effect of Pr_2 on $Nu_2/Ra_2^{1/4}$ for $Pr_1 = 0.7$, $R_t = 0.1$ and various A values is listed in Table 1. The difference of $Nu_2/Ra_2^{1/4}$ between $Pr_2 = 0.7$ and $Pr_2 \to \infty$ is about 17% for $A = 10$. As shown in Fig. 9, these results imply that the effect of Pr_2 is not negligible for $A \geqslant 10$. However, $Nu_2/Ra_2^{1/4}$ is a weak function of Pr_2 for $A \leqslant 1$. Table 1 also shows that the effect of A on $Nu_2/Ra_2^{1/4}$ is much more pronounced than that of Pr_2.

CONCLUSIONS

The present study proposes a more general approach to solve the conjugate problem of laminar natural convection on both sides of a vertical plate. The engineering importance of the present study is that excellent agreements between the present results using the approximation of 1D heat conduction along the plate and experimental data are obtained. This implies that this model has good accuracy for such problems. The present study also shows that the predicted results of Viskanta and Lankford [9] are very close to the present results using the approximation of transverse heat conduction in the plate for smaller values of R_t, such as $R_t \leqslant 0.00103$ (when $A = 1$). However, the present results using the approximation of transverse heat conduction tend to approach those using the approximation of 1D heat conduction along the plate for $A = 1$ when the value of R_t increases, such as $R_t \geqslant 0.0914$. Another conclusion of this study is that the effect of Pr_2 on the heat flux rate through the plate is not negligible for larger values of A. However, its effect is considerably weaker than that of A.

REFERENCES

1. R. Viskanta and M. Abrams, Thermal interaction of two streams in boundary layer flow separated by a wall, *Int. J. Heat Mass Transfer* **14,** 1311–1321 (1971).

2. G. S. H. Lock and R. S. Ko, Coupling through a wall between two free convective systems, *Int. J. Heat Mass Transfer* **16,** 2087–2096 (1973)
3. R. Anderson and A. Bejan, Natural convection on both sides of a vertical wall separating fluids at different temperatures, *ASME J. Heat Transfer* **102,** 630–635 (1980).
4. A. Bejan and R. Anderson, Heat transfer across a vertical impermeable partition imbedded in porous medium, *Int. J. Heat Mass Transfer* **24,** 1237–1245 (1981).
5. A. Bejan and R. Anderson, Natural convection at the interface between a vertical porous layer and an open space, *ASME J. Heat Transfer* **105,** 124–129 (1983).
6. D. Poulikakos, Interaction between film condensation on one side of a vertical wall and natural convection on the other side, *ASME J. Heat Transfer* **108,** 560–566 (1986).
7. A. E. Gill, The boundary layer region for convection in a rectangular cavity, *J. Fluid Mech.* **26,** 515–536 (1966).
8. M. Faghri and E. M. Sparrow, Parallel-flow and counter-flow condensation on an internally cooled vertical tube, *Int. J. Heat Mass Transfer* **23,** 559–562 (1980).
9. R. Viskanta and D. W. Landford, Coupling of heat transfer between two natural convective systems separated by a vertical wall, *Int. J. Heat Mass Transfer* **24,** 1171–1177 (1981).
10. E. M. Sparrow and H. S. Yu, Local non-similarity thermal boundary-layer solution, *ASME J. Heat Transfer* **93,** 328–336 (1971).
11. J. A. Adams and D. F. Rogers, *Computer-Aided Heat Transfer Analysis*. McGraw-Hill, New York (1973).